



Aberystwyth University

Small-Scale Spatial Heterogeneity of Photosynthetic Fluorescence Associated with Biological Soil Crust Succession in the Tengger Desert, China

Lan, Shubin; Thomas, Andrew; Tooth, Stephen; Wu, Li; Hu, Chunxiang

Published in:

Microbial Ecology

DOI:

[10.1007/s00248-019-01356-0](https://doi.org/10.1007/s00248-019-01356-0)

Publication date:

2019

Citation for published version (APA):

Lan, S., Thomas, A., Tooth, S., Wu, L., & Hu, C. (2019). Small-Scale Spatial Heterogeneity of Photosynthetic Fluorescence Associated with Biological Soil Crust Succession in the Tengger Desert, China. *Microbial Ecology*. <https://doi.org/10.1007/s00248-019-01356-0>

General rights

Copyright and moral rights for the publications made accessible in the Aberystwyth Research Portal (the Institutional Repository) are retained by the authors and/or other copyright owners and it is a condition of accessing publications that users recognise and abide by the legal requirements associated with these rights.

- Users may download and print one copy of any publication from the Aberystwyth Research Portal for the purpose of private study or research.
- You may not further distribute the material or use it for any profit-making activity or commercial gain
- You may freely distribute the URL identifying the publication in the Aberystwyth Research Portal

Take down policy

If you believe that this document breaches copyright please contact us providing details, and we will remove access to the work immediately and investigate your claim.

tel: +44 1970 62 2400
email: is@aber.ac.uk

1 **Small-scale spatial heterogeneity of photosynthetic fluorescence associated with biological soil crust**
2 **succession in the Tengger Desert, China**

3 Shubin Lan^{1,2}, Andrew David Thomas², Stephen Tooth², Li Wu^{2,3}, Chunxiang Hu^{1*}

4 ¹ Key Laboratory of Algal Biology, Institute of Hydrobiology, Chinese Academy of Sciences, Wuhan,
5 430072, China

6 ² Department of Geography and Earth Sciences, Aberystwyth University, Aberystwyth, SY23 3DB, UK

7 ³ School of Resources and Environmental Engineering, Wuhan University of Technology, Wuhan, 430072,
8 China

9 * Corresponding author: Tel/Fax.: +86 27 68780866; E-mail address: cxhu@ihb.ac.cn (C.X. Hu)

10

11

12

13

14

15

16

17

18

19

20

21

22

23 **Abstract:** In dryland regions, biological soil crusts (BSCs) have numerous important ecosystem functions.
24 Crust species and functions are, however, highly spatially heterogeneous and remain poorly understood at a
25 range of scales. In this study, chlorophyll fluorescence imaging was used to quantify millimeter-scale
26 patterns in the distribution and activity of photosynthetic organisms in BSCs of different successional
27 stages(cyanobacterial, lichen, moss three main successional stages and three intermix transitional stages)
28 from the Tengger Desert, China. Chlorophyll fluorescence images derived from the Imaging PAM (Pulse
29 Amplitude Modulation) showed that photosynthetic efficiency (including the maximum and effective
30 photosynthetic efficiency, respectively) and fluorescence coverage is significantly different ($P<0.05$)
31 between cyanobacterial, lichen and moss crusts, and that increasing photosynthetically active radiation (PAR)
32 reduced the effective photosynthetic efficiency (Yield). The distribution of photosynthetic organisms in
33 crusts determined Fv/Fm (ratio of variable fluorescence to maximum fluorescence) frequency pattern,
34 although the photosynthetic heterogeneity (*SHI* index) was not significantly different ($P>0.05$) between
35 cyanobacterial and moss crusts, and showed a unimodal pattern of Fv/Fm values. In contrast, photosynthetic
36 heterogeneity was significantly higher ($P<0.05$) in lichen, cyanobacteria-moss and lichen-moss crusts, with
37 a bimodal pattern of Fv/Fm values. Point pattern analysis showed that the distribution pattern of chlorophyll
38 fluorescence varied at different spatial scales and also among the different crust types. These new results
39 provide a detailed (millimeter-scale) insight into crust photosynthetic mechanisms and spatial distribution
40 patterns in different crust types. Collectively, this information provides an improved theoretical basis for
41 crust maintenance and management in dryland regions.

42 **Keywords:** Drylands; biological soil crusts; chlorophyll fluorescence; photosynthesis; heterogeneity;
43 Succession

44

45 **Introduction**

46 Biological soil crusts (BSCs) are widely distributed in dryland regions, and can comprise more than 70% of
47 the living cover in some areas [1, 2]. Within the uppermost millimeters of the soil surface, cyanobacteria,
48 algae, heterotrophic bacteria and micro-fungi cement and bind soil particles to form a complex mosaic BSC
49 layer which exists at the interface of the soil and atmosphere, and thus regulates surface boundary conditions
50 in dryland regions. [3-6]. BSCs play several important roles, which include: i) facilitating soil surface
51 stabilization, fertility and microbial diversity [6-8]; ii) influencing porosity, infiltration and the distribution
52 of water in the soil profile [4, 9, 10]; iii) affecting the process of germination and growth of vascular plants
53 [11]; and iv) providing food and habitat for a variety of soil fauna [12].

54 Heterogeneity is the degree of variation and complexity of processes and patterns in time and space,
55 and is one of the inherent properties of many ecological phenomena [13-15]. It is, however, scale
56 dependent, and the same phenomenon and process when viewed at different scales, may differ significantly
57 [13, 16, 17]. Temporally, different dominant species of photosynthetic organisms appear at different times
58 in the process of BSC succession. Based on the dominant coverage of photosynthetic organisms, BSCs are
59 usually categorized into cyanobacterial crusts (or microalgal or algal crusts), lichen crusts and moss crusts,
60 representing the three main successional stages [2, 4]. Generally, cyanobacterial crusts are the first to form
61 due to the ability of the filamentous cyanobacteria to colonize soil, and so normally represent the early
62 stage of BSCs [3, 18]. Given the right conditions, these crusts can gradually develop and succeed to lichen-
63 and moss-dominated crusts [2, 6, 19-21]. However, in addition to the three main successional stages, there
64 are transitional BSC types and many alternative development scenarios such as cyanobacteria-lichen
65 crusts, cyanobacteria-moss crusts, and lichen-moss crusts [4].

66 At the largest scale, the heterogeneity of BSCs is predominantly controlled by climatic variables, such

67 as temperature and precipitation [22]. At a landscape scale, for instance, climate, geomorphology and biota
68 interact to determine soil physiochemical characteristics, such as soil pH, trace elements and water content,
69 which affect the distribution and succession of BSCs [2, 23, 24]. At the finer patch scale, the characteristics
70 and controls of crust heterogeneity remain poorly understood, although it has been reported that there is a
71 small-scale vertical heterogeneity in BSCs. This vertical heterogeneity may include stratification and
72 physiochemical gradients through the vertical profile of BSCs, with rapid changes in light intensity, pH
73 and oxygen concentration occurring over the millimeter range [4, 5, 23, 25].

74 In dryland regions, BSCs are dry most of the time and therefore they are not metabolically active [21,
75 26]. For instance, in the Tengger desert, it has been found the dominant photosynthetic species
76 (cyanobacteria) are mainly distributed inside the early successional cyanobacterial crust substrate, while in
77 later successional BSCs, the dominant lichens and mosses are directly distributed on the soil surface [26].
78 Consequently, the later successional BSCs are more readily able to use water, even during very small
79 precipitation events [27, 28]. In addition, it has been found that later successional crusts have higher
80 carbon fixation efficiency than early successional ones [26]. In drylands research more generally, there
81 has been increasing interest in photosynthesis and the relative ecological functions of BSCs, but so far
82 most crust samples have been studied in bulk at a relatively coarse (centimeter and upwards) scale.
83 Research is needed at a finer (mm) scale to evaluate the photosynthetic heterogeneity in BSCs and to
84 investigate variations in photosynthetic mechanisms and responses associated with BSC succession.

85 In short, while there has been considerable work in drylands to investigate the influence of
86 heterogeneity and associated resource gradients at large spatial scales (e.g. [29]) and at plant-patch scales
87 (e.g. [30]), there has been limited investigation into variations *within* small BSC patches. Studying
88 heterogeneity at this spatial scale is important because the distribution pattern of photosynthetic organisms

89 in BSCs provides greater insight into crust photosynthetic mechanisms, improves the accuracy of
90 discriminating crust successional stages, and provides an opportunity to establish links between spatial
91 heterogeneity and ecological relevance at a fine scale. Against this backdrop, the overall aim of this study
92 was to use chlorophyll (Chl) fluorescence imaging to visually quantify differences in a range of
93 photosynthetic parameters in BSCs from the Shapotou region of the Tengger Desert, China. The objectives
94 were to: i) investigate how photosynthetic efficiency, coverage and frequency varies with light and crust
95 types; ii) characterise the relationship between photosynthetic spatial heterogeneity and distribution
96 patterns of crust photosynthetic organisms at fine spatial scales; and iii) evaluate the links between
97 photosynthetic heterogeneity and BSC succession.

98

99 **Materials and methods**

100 *Study region and sampling*

101 In this study, BSCs were collected from the Shapotou region of Ningxia Hui Autonomous Region, located
102 on the southeastern edge of the Tengger Desert (37°32'N and 105°02'E; Fig. 1). The study region has a
103 typical continental monsoon climate, and an average elevation of 1339 m. The annual average air
104 temperature is 10.0 °C and the annual average rainfall is approximately 180 mm, falling mainly from June
105 to September, while the annual potential evapotranspiration is more than 2000 mm. The region has large
106 and dense barchan dune chains and reticulate sand dunes. The soil is mainly unconsolidated and nutrient-
107 poor sand that supports a sparse, patchy cover of vascular plants (eg. *Artemisia ordosica* and *Caragana*
108 *korshinskii*) and with BSCs covering more than 80% of soil surface (Fig. 1) [2, 10, 11].

109 Samples were collected from shrub interspaces (at least 0.2 m away from the shrub canopies) with a
110 trowel, and each type of BSCs (including the main successional stages and transitional types; Table 1) was

111 collected from three randomly selected sites. The minimum distance between these sites was over 50 m. At
112 each site, all six types of BSCs were collected at least 5 m apart from each other. Care was taken to ensure
113 the entire thickness of crusts (typically <15 mm) was sampled. All the BSCs were placed into sterilized
114 Petri dishes, and the subsequent analysis was conducted within one month. The main dominant species in
115 BSCs were identified under a microscope according to reference guides [31, 32], and all the analyses were
116 repeated three times.

117

118 *Chlorophyll (Chl) fluorescence imaging*

119 To initiate photosynthetic activity all crust samples (4-5 cm²) were rehydrated with distilled water to
120 saturation, and then placed into a greenhouse (25 ± 2 °C) with light intensity set at 40 μE m⁻² s⁻¹ [33].
121 After 24 hours of photosynthetic recovery, Chl fluorescence parameters of the BSCs were imaged using an
122 Imaging PAM (Pulse Amplitude Modulation; Mini version, Walz, Germany). Before the measurements, all
123 BSCs were dark adapted for at least 10 minutes, then a saturating pulse (approximately 3000 μE m⁻² s⁻¹)
124 was supplied by the Imaging PAM to excite the crust samples. Fluorescence parameters Fo (original
125 fluorescence) and Fm (maximal fluorescence) were automatically recorded, and Fv/Fm (the ratio of
126 variable fluorescence to maximal fluorescence) was also calculated by the Imaging PAM. After
127 measurement of Fv/Fm, the BSCs were illuminated with actinic light at 41, 103 and 249 μE m⁻² s⁻¹. Under
128 each light condition, BSCs were illuminated for at least 3 minutes, and then the saturating pulse was
129 supplied again. During this procedure, fluorescence parameters including Yield (effective quantum yield),
130 qP (photochemical quenching) and qN (non-photochemical quenching) were automatically recorded by the
131 Imaging PAM. Finally, all fluorescence parameters of the different micro-regions of each BSCs were
132 imaged and assigned different colors based on their values to facilitate effective visualization [34].

133

134 ***Photosynthetic coverage and frequency analysis***

135 As an indicator of the photosynthetic activity of photosystem II (PS II), Fv/Fm represents the maximum
136 quantum yield at which light absorbed by PS II is used for reduction of QA (primary quinone acceptor)
137 [34-36]. In this study, crust Fv/Fm was chosen for photosynthetic coverage and frequency analysis, and
138 was also used for the later photosynthetic spatial heterogeneity and point pattern analysis.

139 For photosynthetic coverage and frequency analysis, ten horizontal, equidistant parallel lines were
140 selected from each Fv/Fm image. The coverage of excited Chl fluorescence (Fv/Fm >0.2) [28, 37] and a
141 frequency histogram of the Fv/Fm values were calculated for each selected line. Crust photosynthetic
142 coverage and frequency were then calculated using the selected 10 lines in the Fv/Fm image.

143

144 ***Photosynthetic spatial heterogeneity analysis***

145 On each selected line on the Fv/Fm image, the photosynthetic heterogeneity index (*PHI*) was calculated
146 using the following formula, modified according to the description in Hu and Wang [38]:

147
$$\sum_{i=0}^m [\sum_{j=0}^n |f(2^i, j) - M| / (n+1)] / (m + 1) \quad j + 2^i \leq N$$

148 where $f(2^i, j)$ is the mean of 2^i Fv/Fm values after the j_{th} Fv/Fm value, M is the mean of all the Fv/Fm
149 values on the selected line, N is the number of Fv/Fm values on the line, and m and n are the maximum
150 values of i and j .

151 For the whole crust spatial heterogeneity analysis, ten equidistant parallel lines were selected from the
152 Fv/Fm image in the horizontal and vertical directions, respectively. Then the whole crust *PHI* index was
153 calculated according to the *PHI* indices from each of the selected twenty lines in the Fv/Fm image. The
154 larger the *PHI* index, the greater the photosynthetic heterogeneity of the BSCs.

155

156 ***Point pattern analysis***

157 In each crust Fv/Fm image, a 10×10 mm area of Fv/Fm values was selected to carry out the point pattern
158 analysis. All the Fv/Fm values in the two-dimensional crust image constitute a series of point events, and
159 Ripley's $K(r)$ function was used to reflect the dependency of the point events in spatial pattern [39, 40]:

160
$$K(r) = \lambda^{-1} E[\#(r_{ij} \leq r)]$$

161 where λ is the density of the point events in the research area, E is the expectation of the point events
162 under a certain spatial scale, $\#$ is the number of point events, i and j are the two point events with the same
163 characteristics in the research area, r_{ij} represents the distance from a point to another, and r is the spatial
164 scale.

165 In this study, the function $L(r)$ was used to estimate the distribution pattern of the point events under a
166 certain spatial scale, and was defined as follows [14, 41]:

167
$$L(r) = \sqrt{K(r)/\pi} - r$$

168 At the given spatial scale r , if $L(r) > 0$, the distribution of the point events represents an aggregation
169 pattern; the greater the deviation value, the higher the aggregation intensity. If $L(r) = 0$, the pattern of the
170 point events represents a random distribution, but if $L(r)$ is < 0 , a uniform distribution would be expected
171 [14, 42].

172

173 ***Statistical Analysis and Software***

174 In this study, all the Fv/Fm values in a selected line from the crust Fv/Fm images were acquired using
175 Imaging Win software (Walz, Germany). Among the different developmental and successional BSCs, the
176 variations of each fluorescence parameter, coverage of the excited Chl fluorescence, and PHI index were

177 analyzed by One-Way ANOVA using SPSS 13.0 software (SPSS Inc., USA). In each crust type, the upper
178 and lower envelopes in a random distribution pattern of the function $L(r)$ were calculated by the Monte
179 Carlo simulations of the null model at 99% confidence level using Programita software [14, 41]. The
180 Monte Carlo simulation was conducted 100 times, and if the actual observed point events were higher than
181 the upper envelope, the distribution of the point events was regarded as an aggregation pattern; on the
182 contrary, if the actual observed point events were lower than the lower envelope, the pattern was
183 considered to be a uniform distribution.

184

185 **Results**

186 *Photosynthetic efficiency in BSCs*

187 In this study, three main successional stages of BSCs were sampled, including cyanobacterial crusts,
188 lichen crusts and moss crusts (Table 1). The dominant species in cyanobacterial crusts were *Microcoleus*
189 *vaginatus*, while *Collema* sp. and *Bryum* sp. dominated in lichen and moss crusts, respectively (Table 1).
190 *Microcoleus vaginatus* was found in substrate soils, and few other photosynthetic organisms were found on
191 the surface of cyanobacterial crusts (Fig. 2A). The coverage of *Collema* sp. occupied more than 70% of the
192 surface area of lichen crusts during dry periods, increasing up to 100% when the crust surface was
193 moistened (Fig. 2B). *Bryum* sp. almost completely covered the surface area of moss crusts even during dry
194 periods (Fig. 2C). Consequently, there was clear photosynthetic variation between the different
195 successional stages of BSCs. Although the Fv/Fm values appear as blue fluorescence images in all three
196 main successional stages (Fig. 2D, E, F), Fv/Fm increased significantly from cyanobacterial crusts to
197 lichen crusts and to moss crusts ($P < 0.05$).

198 Under different PAR conditions (41, 103 and 249 $\mu\text{E m}^{-2} \text{s}^{-1}$), fluorescence parameters including

199 Yield, qP and qN were displayed in the form of false color images (Fig. 3). With the increase in PAR, both
200 crust Yield and qP decreased, indicated by the color changing from blue to green and purple to blue-purple,
201 respectively. By contrast, with the increase in PAR, the color of qN changed from orange to yellow-green
202 or yellow-green to blue-violet, although there was no statistically significant increase in the parameter
203 value ($P>0.05$; Fig. S1). In addition, fluorescence parameters Yield and qP were significantly different on
204 the different successional BSCs ($P<0.05$), but no significant difference was found in the fluorescence
205 parameter qN ($P>0.05$; Fig. 3).

206 In addition to the main successional stages of BSCs, three transitional crust types were also sampled,
207 including cyanobacteria-lichen crusts, cyanobacteria-moss crusts, and lichen-moss crusts (Fig. 4; Table 1).
208 In cyanobacteria-lichen and cyanobacteria-moss crusts, the coverage of lichens and mosses were all $<30\%$,
209 while in lichen-moss crusts, the coverage of lichens and mosses was $>40\%$, respectively (Table 1). All the
210 transitional stage BSC Fv/Fm values were not significantly different (between 0.68 and 0.71; $P>0.05$; Fig.
211 S2), and presented blue false color fluorescence images (Fig. 4), . False color images of Yield, qP and qN
212 of the three transitional BSCs under PAR conditions of $41\mu\text{E m}^{-2}\text{ s}^{-1}$ were also produced (Fig. 4). The
213 color of Yield was blue (although numerically less than Fv/Fm), qP was purple, and qN was yellow-green
214 (Fig. 4). There were no significant differences among the different transitional stages of BSCs ($P>0.05$);
215 values were 0.63-0.66 for Yield, 0.77-0.81 for qP, and 0.19-0.36 for qN (Fig. S2).

216

217 *Photosynthetic coverage and frequency in BSCs*

218 Although all BSCs were rich in photosynthetic organisms, there were significant differences in
219 fluorescence within the crusts (Figs. 2 and 3). The Chl fluorescence coverage was low in cyanobacterial
220 crusts and lichen crusts, but covered almost the entire moss crusts (Figs. 3F and 5A). With the succession

221 of BSCs, the proportion of lichens and mosses increased gradually, and Chl fluorescence responses
222 increased correspondingly ($P < 0.05$; Fig. 5A). In cyanobacterial crusts, the frequency of Fv/Fm showed a
223 unimodal pattern, and could be roughly divided into three groups: i) a no fluorescence signal group where
224 Fv/Fm = 0 over much of the crusts; ii) a Fv/Fm value greater than 0.7 group over only a small part of the
225 crusts; and iii) a group where the frequency of Fv/Fm values over the crust fluctuated within a small range
226 (Fig. 6A). In lichen crusts, the frequency of Fv/Fm values showed a bimodal pattern, with peaks at Fv/Fm
227 = 0 and 0.6-0.7 (Fig. 6B). In moss crusts, the frequency of Fv/Fm values showed a unimodal pattern with a
228 peak of Fv/Fm greater than 0.7 (Fig. 6C). In the three transitional BSCs, the frequency of Fv/Fm values
229 showed a similar bimodal pattern to that in lichen crusts (Fig. 6D, E, F).

230

231 ***Photosynthetic spatial heterogeneity and distribution pattern in BSCs***

232 The heterogeneity of Chl fluorescence (*SHI* index) was not significantly different ($P > 0.05$) between
233 cyanobacterial crusts and moss crusts, but it was significantly lower in cyanobacterial and moss crusts
234 compared to lichen crusts ($P < 0.05$; Fig. 5B). Among the three transitional stages of BSCs, the *SHI* index of
235 Chl fluorescence was the lowest in the cyanobacteria-lichen crusts, and similar to the indices in
236 cyanobacterial crusts and moss crusts ($P > 0.05$; Fig. 5B). In contrast, the spatial heterogeneity of Chl
237 fluorescence was significantly higher in cyanobacteria-moss and lichen-moss crusts compared to the other
238 crust types ($P < 0.05$; Fig. 5B).

239 According to the observed Fv/Fm point events relative to the upper and lower envelopes of the
240 function $L(r)$, the distribution pattern of Chl fluorescence can be clearly determined. The point pattern
241 analysis showed that the distribution pattern of Chl fluorescence changed at different spatial scales, and
242 also between the different crust types (Fig. 7). In cyanobacterial crusts, Chl fluorescence showed an

243 aggregation pattern at a spatial scale of 0-1.7 mm but a random distribution at a scale of 1.7-2.5 mm. In the
244 other crust types, all Chl fluorescence showed an aggregation pattern at a spatial scale of 0-2.5 mm, but a
245 tendency for a change from an aggregation to a more random distribution appeared in cyanobacteria-lichen
246 and lichen crusts (Fig. 7).

247

248 **Discussion**

249 Light energy absorbed by Chl molecules can be used to drive photochemical reactions but alternatively can
250 be lost as Chl fluorescence or dissipated as heat [36]. A change in Chl fluorescence is likely related to a
251 variation of photochemical efficiency in photosynthetic organisms [26, 36]. Therefore, Chl fluorescence
252 technology has been widely used in physiological and ecological research into cyanobacteria [33], lichens
253 [34], higher plants [35], and also BSCs [26]. In this study, we used a Chl fluorescence imaging technique
254 to investigate fine-scale photosynthetic spatial heterogeneity in different BSCs types, in order to provide
255 more information on crust photosynthetic mechanisms.

256

257 *Imaging photosynthetic efficiency variation in BSCs*

258 Imaging PAM presents Chl fluorescence signals in the form of a false color image, which reflects the
259 photosynthetic heterogeneity and distribution pattern in BSCs. The composition of photosynthetic
260 organisms changes with the succession of BSCs [8, 43], thus leading to distinctive imaging of Chl
261 fluorescence signals excited from different crust types (Figs. 2 and 4). Compared with other Chl
262 fluorescence detectors (such as Plant Efficiency Analyzer; PEA), imaging Chl fluorescence using Imaging
263 PAM can show photosynthetic activity in BSCs in greater detail at finer scales. This helps improve our
264 understanding of the fine scale distribution and functions of BSCs. In our study region the basic spatial

265 elements (photoautotrophic organisms) are cyanobacteria, lichens and mosses. Therefore, we can regard
266 the whole region BSCs as comprising three different types, dominated by cyanobacteria, lichens or mosses,
267 respectively.

268 Photosynthetic performance at fine scales is reflected by the adaptation of PS II of the photosynthetic
269 organisms residing in BSCs. The Fv/Fm ratio reflects the largest solar energy conversion efficiency in the
270 PS II reaction center, and is expected to decrease under environmental stresses such as desiccation [26, 34].
271 However, in unstressed conditions (e.g. when crusts are hydrated), Fv/Fm is maintained at a relatively
272 stable level. Furthermore, our results reveal that the Fv/Fm gradually increased with the succession from
273 cyanobacterial crusts to lichen crusts and to moss crusts ($P < 0.05$), which indicates that the maximum
274 photosynthetic efficiency is higher in the later successional BSCs. Under a given light condition, Yield
275 reflects the effective photosynthetic efficiency (quantum yield) of PS II when parts of the PS II reaction
276 centers are closed [34, 36]. Therefore, Yield was lower than Fv/Fm, and decreased gradually with
277 increasing PAR (Fig. 3). Similarly, qP also decreased with increasing PAR (although the decrease in
278 cyanobacterial crusts was not statistically significant; $P > 0.05$), reflecting a decrease in the ratio of open PS
279 II centers. With decreases of Yield and qP, the non-photochemical quenching parameter qN was expected
280 to increase, so that more light energy could be quenched in non-photochemical form. This is because when
281 PAR is within a certain range, BSCs can maintain the stability of qP by increasing qN [36, 45]. However,
282 in our study, as PAR increased from 41 to 249 $\mu\text{E m}^{-2} \text{s}^{-1}$, the increase of qN was still limited. Similar to
283 Fv/Fm, Yield and qP also gradually increased with the crust succession, although no significant difference
284 was found in the fluorescence parameter qN. This is further evidence that photosynthetic efficiency is
285 stronger in the later successional BSCs.

286

287 ***Photosynthetic spatial heterogeneity in BSCs***

288 Although a variety of fluorescence parameters were measured in our study, in reality all the fluorescence
289 parameters were excited from the same photosynthetic organisms in each BSCs, so that all the fluorescence
290 parameters exhibited the same spatial distribution characteristics. In the present study, Fv/Fm was used to
291 characterise the photosynthetic heterogeneity and spatial distribution pattern. In cyanobacterial crusts,
292 photosynthetic spatial heterogeneity may be affected by the uneven distribution of cyanobacterial filaments
293 not only on the surface but also at depth because most cyanobacteria reside in the surface substrate (the
294 exception being some species with strong radiation-protective ability, such as *Scytonema* and *Nostoc*) [4,
295 5]. The incident light in such crusts is rapidly attenuated by the soil particles and exopolymeric matrix
296 before it excites the cyanobacteria [23, 44]; in turn, the excited fluorescence signals are similarly
297 attenuated before they can be detected by the Imaging PAM, which eventually leads to the low
298 photosynthetic fluorescence coverage and unimodal pattern of Fv/Fm = 0 in cyanobacterial crusts (Figs.
299 5A and 6A).

300 As BSCs succeed, the position of dominant photosynthetic organisms changes from the substrate to
301 the surface. Lichens are the symbionts of cyanobacteria (or algae in some lichens) and fungi, so the Chl
302 fluorescence signals of lichen crusts in reality were excited from the symbiotic cyanobacteria. These
303 cyanobacteria are covered by fungi and also large quantities of exopolymeric matrix, so most symbiotic
304 cyanobacteria in the lichen crusts are not directly exposed to the air [46], which leads to significant
305 attenuation of incident light. Similarly, the fluorescence signals excited from the symbiotic cyanobacteria
306 by the attenuated incident light are further attenuated before the Imaging PAM can detect them. In our
307 study, no fluorescence signal was excited in most micro-regions of lichen crusts (Fig. 5A). However, the
308 frequency of Fv/Fm with high values (>0.6) was significantly higher than the frequency with other values

309 (except $F_v/F_m = 0$) in lichen crusts, and thus the frequency of F_v/F_m was bimodal (Fig. 6B).

310 In moss crusts, mosses are not only directly distributed on the crust surface, but also directly accept
311 incident light and the excited fluorescence signals could be directly detected by the Imaging PAM.
312 Therefore, the excited fluorescence covered almost the entire moss crusts, and most of the F_v/F_m values
313 were high (>0.6) and unimodal (Fig. 6C).

314 In summary, the heterogeneity of Chl fluorescence can be attributed to the heterogeneous distribution
315 of photosynthetic organisms in BSCs, which also reflects differences in successional stage of BSCs in
316 different micro-regions. In the present study, the photosynthetic heterogeneity index *PHI* ranged from 0.02
317 to 0.17 among the different BSC types, with the highest values in cyanobacteria-moss and lichen-moss
318 crusts (Fig. 5B).

319

320 *Photosynthetic spatial scale associated with crust succession*

321 Our results confirm that crust heterogeneity is a common phenomenon, and that it varies with spatial scale.
322 In cyanobacterial crusts, the results suggested cyanobacterial distribution changed from aggregation to
323 random with the increasing spatial scale; while in lichen and moss crusts, all the photosynthetic organisms
324 aggregated throughout the experimental spatial scale (0-2.5 mm), although there was a tendency for a
325 change to a more random distribution pattern in lichen crusts (Fig. 7B). However, due to the size
326 limitations of the mini Imaging PAM used in this study, the spatial scale was limited in 2.5 mm, so it is not
327 clear if the tendency towards a random distribution persisted as spatial scale increased. Using the Max
328 version of Imaging PAM or other equipment will help us understand the heterogeneous distribution of
329 BSCs in even greater detail and provide more direct evidence of the heterogeneous distribution of BSCs at
330 larger scales.

331 There are parallels between the controls over small-scale photosynthetic heterogeneity within BSCs
332 and variations in BSCs cover over larger regions where water availability, effective incidence of light
333 under micro-topography and other physicochemical conditions affect crust distribution [6, 19-21].
334 Together, variations at all scales add spatial heterogeneity and ecological diversity to the landscape. Chl
335 fluorescence technology can not only detect the landscape-scale distribution of photosynthetic organisms
336 and the associated spatial heterogeneity, but also provides a useful approach for monitoring environmental
337 conditions and diagnosing photosynthetic change [47], which ultimately may inform the maintenance and
338 management of healthy BSCs. Using Chl fluorescence technology in field settings removes the need for
339 crust destruction, and also provides a good proxy for Chl-a content [26]. Furthermore, the present study
340 reveals that Chl fluorescence imaging can clearly provide a more accurate indication about crust
341 succession at a fine scale.

342 The results presented in this study and published elsewhere (e.g. [26, 48]) all support the idea that
343 later successional BSCs have higher photosynthetic efficiency than earlier stages, and are likely to have a
344 greater range of ecological functions (e.g. carbon and nitrogen fixation). Various techniques could
345 therefore be used to accelerate the succession of BSCs in a bid to mitigate against a range of land
346 degradation processes [3, 18, 49, 50]. For example, a large scale, straw checkerboard technique was used
347 successfully in the study region from 1956 to promote the development and succession of BSCs [51].
348 Measures are also needed to ensure that BSCs are not overly disturbed (e.g. by maintaining well managed
349 grazing regimes) [52], because disturbance could convert later to early successional BSCs, thus
350 representing a significant loss of photosynthetic carbon fixation and other relevant ecological functions
351 [22, 48].

352

353 **Conclusion**

354 In this study, a novel Chl fluorescence imaging technique was used to investigate the photosynthetic
355 heterogeneity of different crust types found in the Tengger Desert, China. The results show that with crust
356 succession, maximum photosynthetic efficiency (Fv/Fm after dark adaptation) gradually increased, and
357 fluorescence coverage also increased correspondingly. Under light conditions, although effective
358 photosynthetic efficiency decreased with the increasing PAR, it increased with crust succession.
359 Cyanobacterial crusts and moss crusts showed the two extremes of photosynthetic coverage, being mostly
360 low and mostly high, respectively, but both displayed the same unimodal Fv/Fm frequency. The
361 heterogeneity (*SHI* index) was not significantly different ($P > 0.05$) between cyanobacterial and moss crusts
362 but was higher in lichen crusts ($P < 0.05$), which had a bimodal pattern of Fv/Fm frequency. Point pattern
363 analysis showed that distribution patterns of Chl fluorescence varied at different spatial scales and among
364 the different crust types. This implies that when assessing crust photosynthetic performance, such as its role
365 in carbon fixation and storage, in addition to consideration of BSC succession, it is still necessary to consider
366 the impact of scale, particularly the heterogeneity of BSCs. In-depth understanding of the characteristics of
367 photosynthetic heterogeneity and the complexity of landscapes at different scales will provide further
368 insights into crust development and succession, and enable more accurate assessment of photosynthetic
369 carbon fixation, storage and other ecological functions through the up-scaling of heterogeneous ground-
370 based data.

371

372 **Acknowledgements**

373 This study was kindly supported by the Strategic Priority Research Program of the Chinese Academy of
374 Sciences (No. XDA17010502), National Natural Science Foundation of china (Nos. 31670456 and

375 31300322), Youth Innovation Promotion Association CAS (No. 2017385) and European Union's Horizon
376 2020 research and innovation programme under the Marie Skłodowska-Curie Grant (No. 663830). The paper
377 was prepared while S. Lan was a Sêr Cymru Fellow at Aberystwyth University, and L. Wu was a Visiting
378 Scholar at Aberystwyth University.

379

380 **References**

- 381 1. Hu C, Gao K, Whitton, BA (2012) Semi-arid Regions and Deserts. In: Whitton, B.A., Ed. Ecology of
382 Cyanobacteria II: Their Diversity in Space and Time. Springer Science+Business Media, Dordrecht,
383 pp 345-369.
- 384 2. Lan S, Wu L, Zhang D, Hu C (2015) Analysis of environmental factors determining development and
385 succession in biological soil crusts. *Sci Total Environ* 538:492-499.
- 386 3. Hu C, Liu Y, Song L, Zhang D (2002) Effect of desert soil algae on the stabilization of fine sands. *J*
387 *Appl Phycol* 14:281-292.
- 388 4. Lan S, Wu L, Zhang D, Hu C (2012) Successional stages of biological soil crusts and their
389 microstructure variability in Shapotou region (China). *Environ Earth Sci* 65(1):77-88.
- 390 5. Hu C, Zhang D, Huang Z, Liu Y (2003) The vertical microdistribution of cyanobacteria and green
391 algae within desert crusts and the development of the algal crusts. *Plant Soil* 257 :97-111.
- 392 6. Lan S, Zhang Q, Wu L, Liu Y, Zhang D, Hu C (2014) Artificially Accelerating the Reversal of
393 Desertification: Cyanobacterial Inoculation Facilitates the Succession of Vegetation Communities.
394 *Environ Sci Technol* 48:307-315.
- 395 7. Belnap J, Gillette DA (1998) Vulnerability of desert biological soil crusts to wind erosion: the
396 influences of crust development, soil texture, and disturbance. *J Arid Environ* 39(2):133-142.

- 397 8. Elliott DR, Thomas AD, Hoon SR, Sen R (2014) Niche partitioning of bacterial communities in
398 biological crusts and soils under grasses, shrubs and trees in the Kalahari. *Biodivers Conserv* 23:1709-
399 1733.
- 400 9. Eldridge DJ, Zaady E, Shachak M (2000) Infiltration through three contrasting biological soil crusts in
401 patterned landscapes in the Negev, Israel. *Catena* 40:323-336.
- 402 10. Lan S, Hu C, Rao B, Wu L, Zhang D, Liu Y (2010) Non-rainfall water sources in the topsoil and their
403 changes during formation of man-made algal crusts at the eastern edge of Qubqi Desert, Inner Mongolia.
404 *Sci China Life Sci* 53:1135-1141.
- 405 11. Li X, Jia X, Long L, Zerbe S (2005) Effects of biological soil crusts on seed bank, germination and
406 establishment of two annual plant species in the Tengger Desert (N China). *Plant Soil* 277:375-385.
- 407 12. Li X, Jia R, Chen Y, Huang L, Zhang P (2011) Association of ant nests with successional stages of
408 biological soil crusts in the Tengger Desert, Northern China. *Appl Soil Ecol* 47:59-66.
- 409 13. Pickett STA, Cadenasso ML (1995) Landscape ecology: Spatial heterogeneity in ecological systems.
410 *Science* 269:331-334.
- 411 14. Wiegand T, Moloney KA (2004) Rings, circles and null-models for point pattern analysis in ecology.
412 *Oikos* 104:209-229.
- 413 15. Shen G, He F, Waagepetersen R, Sun I, Hao Z, Chen Z, Yu M (2013) Quantifying effects of habitat
414 heterogeneity and other clustering processes on spatial distributions of tree species. *Ecology*
415 94(11):2436-2443.
- 416 16. Bowker MA, Belnap J, Davidson DW, Goldstein H (2006) Correlates of biological soil crust abundance
417 across a continuum of spatial scales: Support for a hierarchical conceptual model. *J Appl Ecol* 43 :152-
418 163.

- 419 17. Baillod AB, Tschamtké T, Clough Y, Batáry P (2017) Landscape-scale interactions of spatial and
420 temporal cropland heterogeneity drive biological control of cereal aphids. *J Appl Ecol* 54:1804-1813.
- 421 18. Liu Y, Cockell CS, Wang G, Hu C, Chen L, De Philippis R (2008) Control of Lunar and Martian Dust-
422 Experimental Insights from Artificial and Natural Cyanobacterial and Algal Crusts in the Desert of
423 Inner Mongolia, China. *Astrobiology* 8 :75-86.
- 424 19. Zaady E, Kuhn U, Wilske B, Sandoval-Soto L, Kesselmeier J (2000) Patterns of CO₂ exchange in
425 biological soil crusts of successional age. *Soil Biol Biochem* 32:959-966.
- 426 20. Zaady E, Karnieli A, Shachak M (2007) Applying a field spectroscopy technique for assessing
427 successional trends of biological soil crusts in a semi-arid environment. *J Arid Environ* 70:463-477.
- 428 21. Kidron GJ, Vonshak A, Abeliovich A (2008) Recovery rates of microbiotic crusts within a dune
429 ecosystem in the Negev Desert. *Geomorphology* 100:444-452.
- 430 22. Viles HA (2008) Understanding dryland landscape dynamics: do biological crusts hold the key?
431 *Geography Compass* 2(3):899-919.
- 432 23. Garcia-Pichel F, Belnap J (1996) Microenvironments and microscale productivity of cyanobacterial
433 desert crusts. *J Phycol* 32:774-782.
- 434 24. Bowker MA, Belnap J, Davidson DW, Phillips SL (2005) Evidence for micronutrient limitation of
435 biological soil crusts: Importance to arid-lands restoration. *Ecol Appl* 15:1941-1951.
- 436 25. Abed RMM, Lam P, De Beer D, Stief P (2013) High rates of denitrification and nitrous oxide emission
437 in arid biological soil crusts from the Sultanate of Oman. *ISME J* 7:1862-1875.
- 438 26. Lan S, Wu L, Zhang D, Hu C (2017) Biological soil crust community types differ in photosynthetic
439 pigment composition, fluorescence and carbon fixation in Shapotou region of China. *Appl Soil Ecol*
440 111:9-16.

- 441 27. Wu L, Lan S, Zhang D, Hu C (2011) Small-scale Vertical Distribution of Algae and Structure of Lichen
442 Soil Crusts. *Microbial Ecol* 62:715-724.
- 443 28. Wu L, Lan S, Zhang D, Hu C (2013) Functional reactivation of photosystem II in lichen soil crusts
444 after long-term desiccation. *Plant Soil* 369:177-186
- 445 29. Swap RJ, Annegarn HJ, Suttles JT, et al (2002) The Southern African Regional Science Initiative
446 (SAFARI 2000): Overview of the Dry Season Field Campaign. *S Afr J Sci* 98(3):125-130.
- 447 30. Dean WRJ, Milton SJ, Jeltsch F (1999) Large trees, fertile islands, and birds in arid savanna. *J Arid*
448 *Environ* 41:61-78.
- 449 31. Hu H, Li R, Wei Y, Zhu H, Chen J, Shi Z (1980) *Freshwater Algae in China*. Shanghai Science and
450 Technology Press, Shanghai (in Chinese).
- 451 32. Rosentreter R, Bowker M, Belnap J (2007) *A Field Guide to Biological Soil Crusts of Western U.S.*
452 *Drylands*. U.S. Government Printing Office, Denver
- 453 33. Ohad I, Raanan H, Keren N, Tchernov D, Kaplan A (2010) Light-induced changes within photosystem
454 II protects *Microcoleus* sp. in biological desert sand crusts against excess light. *PLoS ONE* 5(6):e11000.
- 455 34. Wu L, Lei Y, Lan S, Hu C (2017) Photosynthetic recovery and acclimation to excess light intensity in
456 the rehydrated lichen soil crusts. *PLoS ONE* 12(3):e0172537.
- 457 35. Heber U, Bilger W, Shuvalov VA (2006) Thermal energy dissipation in reaction centres and in the
458 antenna of photosystem II protects desiccated poikilohydric mosses against photo-oxidation. *J Exp Bot*
459 57:2993-3006.
- 460 36. Baker NR (2008) Chlorophyll fluorescence: a probe of photosynthesis in vivo. *Annu Rev Plant Biol*
461 59:89-113.
- 462 37. Green TGA, Schlensog M, Sancho LG, Winkler JB, Broom FD, Schroeter B (2002) The photobiont

463 determines the pattern of photosynthetic activity within a single lichen thallus containing
464 cyanobacterial and green algal sectors (photosymbiodeme). *Oecologia* 130:191-198.

465 38. Hu H, Wang X (2008) Unified index to quantifying heterogeneity of complex networks. *Physica A*
466 387(14):3769-3780.

467 39. Ripley BD (1976) The second-order analysis of stationary point processes. *J Appl Probab* 13:255-266.

468 40. Shi P, Ge F, Yang Q, Wang J (2009) A new algorithm of the edge correction in the point pattern
469 analysis and its application. *Acta Ecologica Sinica* 29(2) :804-809.

470 41. Wiegand T, Moloney KA (2014) A handbook of spatial point pattern analysis in ecology. Chapman and
471 Hall/CRC press, Boca Raton, FL.

472 42. Law R, Illian J, Burslem DFRP, Gratzner G, Gunatilleke CVS, Gunatilleke IAUN (2009) Ecological
473 information from spatial patterns of plants: insights from point process theory. *J Ecol* 97:616-628.

474 43. Lan S, Wu L, Zhang D, Hu C (2013) Assessing Level of Development and Successional Stages in
475 Biological Soil Crusts with Biological Indicators. *Microbial Ecol* 66:394-403.

476 44. Mugnai G, Rossi F, Felde VJ, Colesie C, Büdel B, Peth S, Kaplan A, De Philippis R (2018).
477 Development of the polysaccharidic matrix in biocrusts induced by a cyanobacterium inoculated in
478 sand microcosms. *Biol Fert Soils* 54:27-40.

479 45. Müller P, Li X, Niyogi KK (2001) Non-Photochemical Quenching. A Response to Excess Light Energy.
480 *Plant Physiol* 125:1558-1566.

481 46. Wu L, Zhang G, Lan S, Zhang D, Hu C (2013) Microstructures and photosynthetic diurnal changes in
482 the different types of lichen soil crusts. *Eur J Soil Biol* 59:48-53.

483 47. Lan S, Wu L, Zhang D, Hu C (2012) Composition of photosynthetic organisms and diurnal changes of
484 photosynthetic efficiency in algae and moss crusts. *Plant Soil* 351:325-336.

485 48. Housman DC, Powers HH, Collins AD, Belnap J (2006) Carbon and nitrogen fixation differ between
486 successional stages of biological soil crusts in the Colorado Plateau and Chihuahuan Desert. *J Arid*
487 *Environ* 66:620-634.

488 49. Bowker MA, Reed SC, Belnap J, Phillips SL (2002) Temporal variation in community composition,
489 pigmentation, and Fv/Fm of desert cyanobacterial soil crusts. *Microbial Ecol* 43:13-25.

490 50. Belnap J (1993) Recovery rates of cryptobiotic crusts: Inoculant use and assessment methods. *Great*
491 *Basin Nat* 53:89-95.

492 51. Li X, Xiao H, He M, Zhang J (2006) Sand barriers of straw checkerboards for habitat restoration in
493 extremely arid desert regions. *Ecol Eng* 28:149-157.

494 52. Thomas AD (2012) Impact of grazing intensity on seasonal variations in SOC and soil CO₂ efflux in
495 two semiarid grasslands in southern Botswana. *Philos T Roy Soc B* 367:3076-3086.

496

497

498

499

500

501

502

503

504

505

506

507 **Figure captions:**

508 **Fig. 1** Location of the study region (left) and example of the characteristic patches of vascular plants and
509 BSCs on the Tengger Desert margins in the Shapotou region (right).

510 **Fig. 2** The three main successional stages of BSCs in the Shapotou region, including cyanobacterial crusts
511 (A), lichen crusts (B) and moss crusts (C), and their fluorescence images (Fv/Fm) in (D), (E), (F),
512 respectively. The images are in false color, and the color scale on each Fv/Fm image represents the values
513 from 0 (red) to 1 (purple).

514 **Fig. 3** Comparison of fluorescence parameters Yield, qP and qN in the three main successional stages of
515 BSCs. (A), (B) and (C) show the comparison of the values of three parameters under different PAR
516 conditions; for a given PAR condition, values with different letters indicate that the difference is significant
517 at the 0.05 level ($P < 0.05$). Cyanobacterial crusts (D), lichen crusts (E) and moss crusts (F) show the
518 fluorescence images of three parameters under different PAR conditions (from left to right, 41, 103 and 249
519 $\mu\text{E m}^{-2} \text{s}^{-1}$). The images in (D), (E) and (F) are in false color, and the color scale on each image represents
520 the values from 0 (red) to 1 (purple).

521 **Fig. 4** Three transitional stages of BSCs in the Shapotou region, including cyanobacteria-lichen crusts (A),
522 cyanobacteria-moss crusts (B) and lichen-moss crusts (C), and their fluorescence images including Fv/Fm,
523 Yield, qP and qN. The Yield, qP and qN were determined under the PAR condition of 41 $\mu\text{E m}^{-2} \text{s}^{-1}$. The
524 images are in false color, and the color scale on each image represents the values from 0 (red) to 1 (purple).

525 **Fig. 5** Box and whisker plots of fluorescence coverage (A) and spatial heterogeneity index (B) in the different
526 successional stages of BSCs (see Table 1 for the definition of abbreviations). For each parameter, the values
527 with different letters indicate that the difference is significant at the 0.05 level ($P < 0.05$).

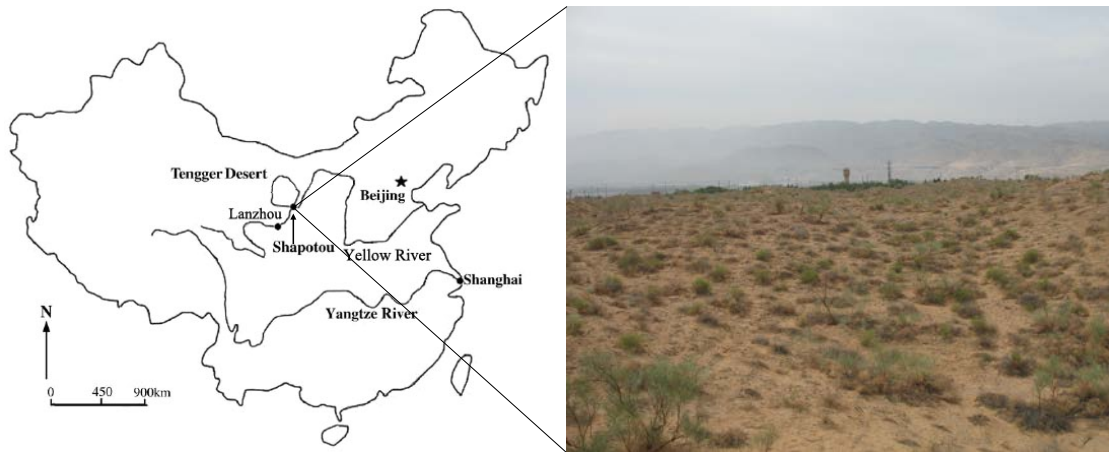
528 **Fig. 6** Frequency histogram of Fv/Fm intervals in the different successional stages of BSCs, including

529 cyanobacterial crusts (A), lichen crusts (B), moss crusts (C), cyanobacteria-lichen crusts (D), cyanobacteria-
530 moss crusts (E) and lichen-moss crusts (F).

531 **Fig. 7** Point pattern analysis of Chl fluorescence in the different successional stages of BSCs, including
532 cyanobacterial crusts (A), lichen crusts (B), moss crusts (C), cyanobacteria-lichen crusts (D), cyanobacteria-
533 moss crusts (E) and lichen-moss crusts (F). The solid and dotted lines in the figure show the envelopes in
534 the random distribution pattern of the function $L(r)$ and the observed fluorescence values, respectively.

535
536
537
538
539
540
541
542
543
544
545
546
547
548
549
550
551
552
553
554
555
556

557 **Fig. 1**



558

559

560

561

562

563

564

565

566

567

568

569

570

571

572

573

574

575

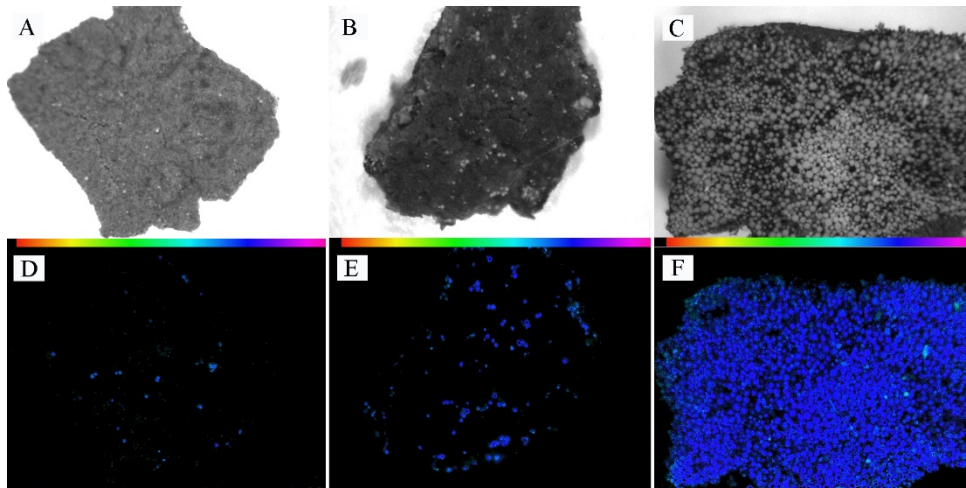
576

577

578

579

580 **Fig. 2**



581

582

583

584

585

586

587

588

589

590

591

592

593

594

595

596

597

598

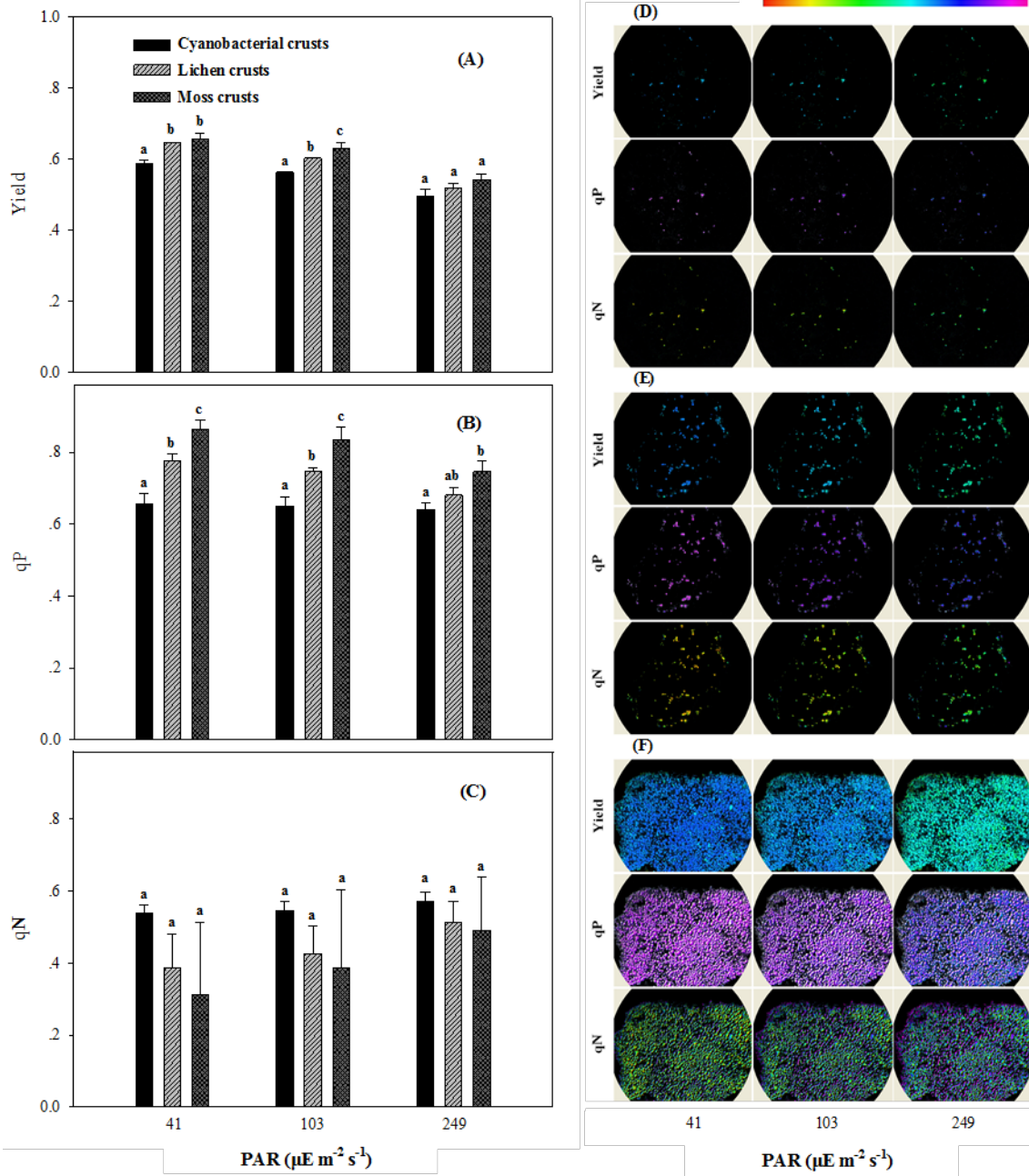
599

600

601

602

603 **Fig. 3**



604

605

606

607

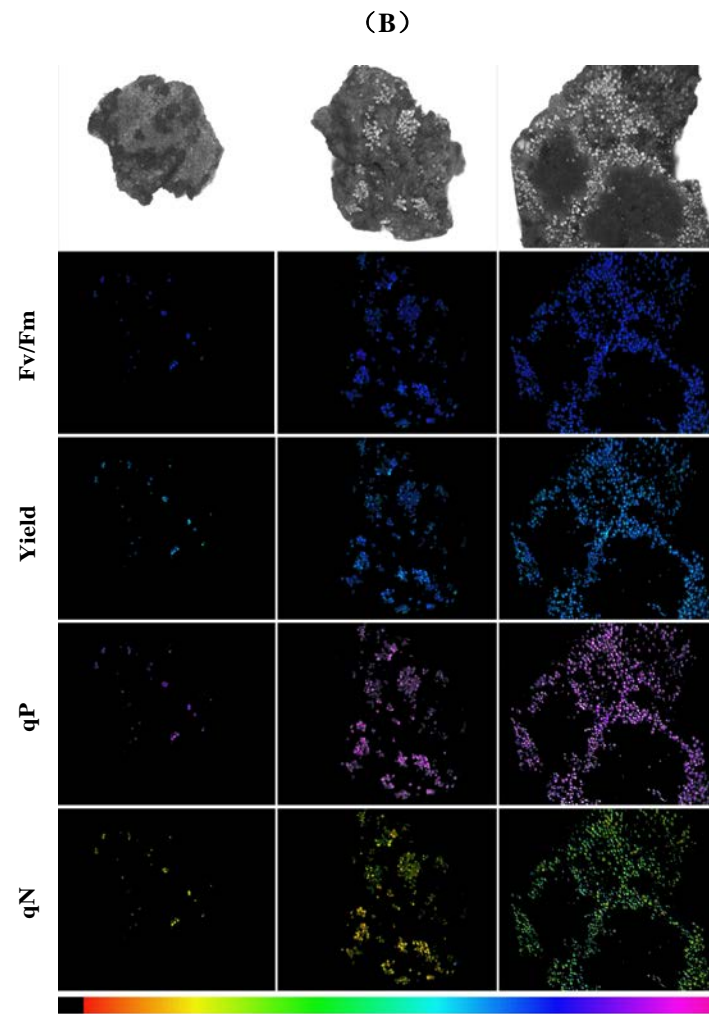
608

609

610

611

612 Fig. 4



613

614

615

616

617

618

619

620

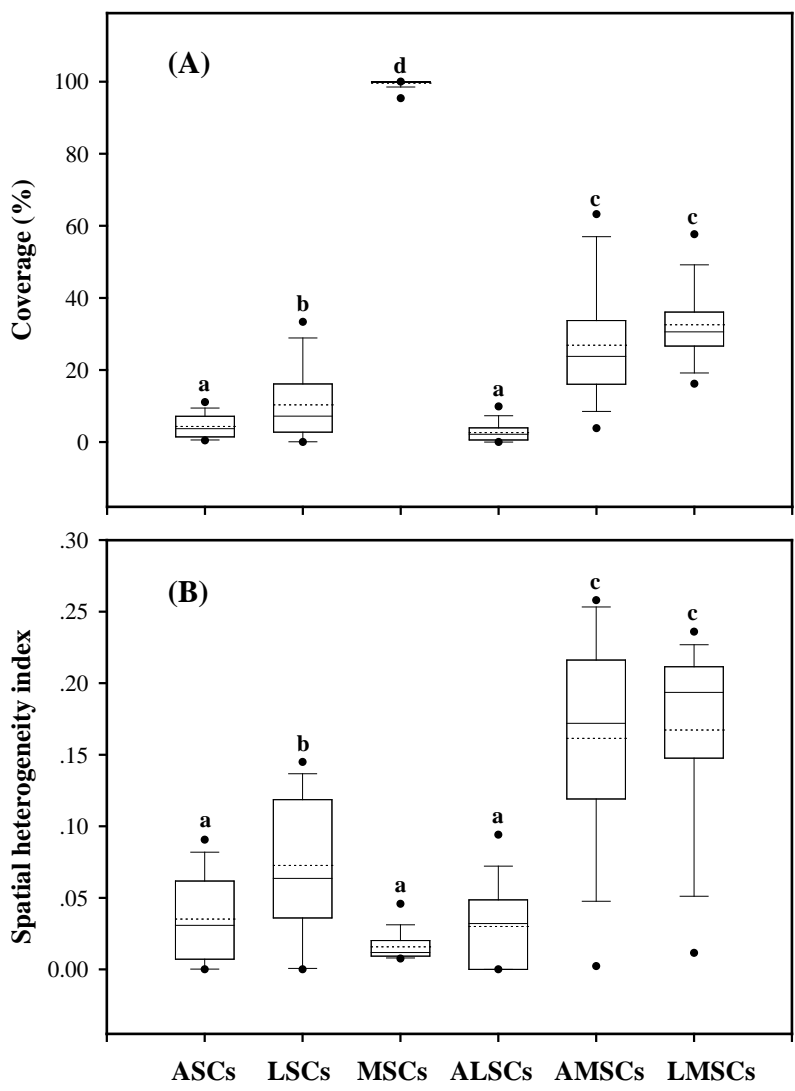
621

622

623

624

625



627

628

629

630

631

632

633

634

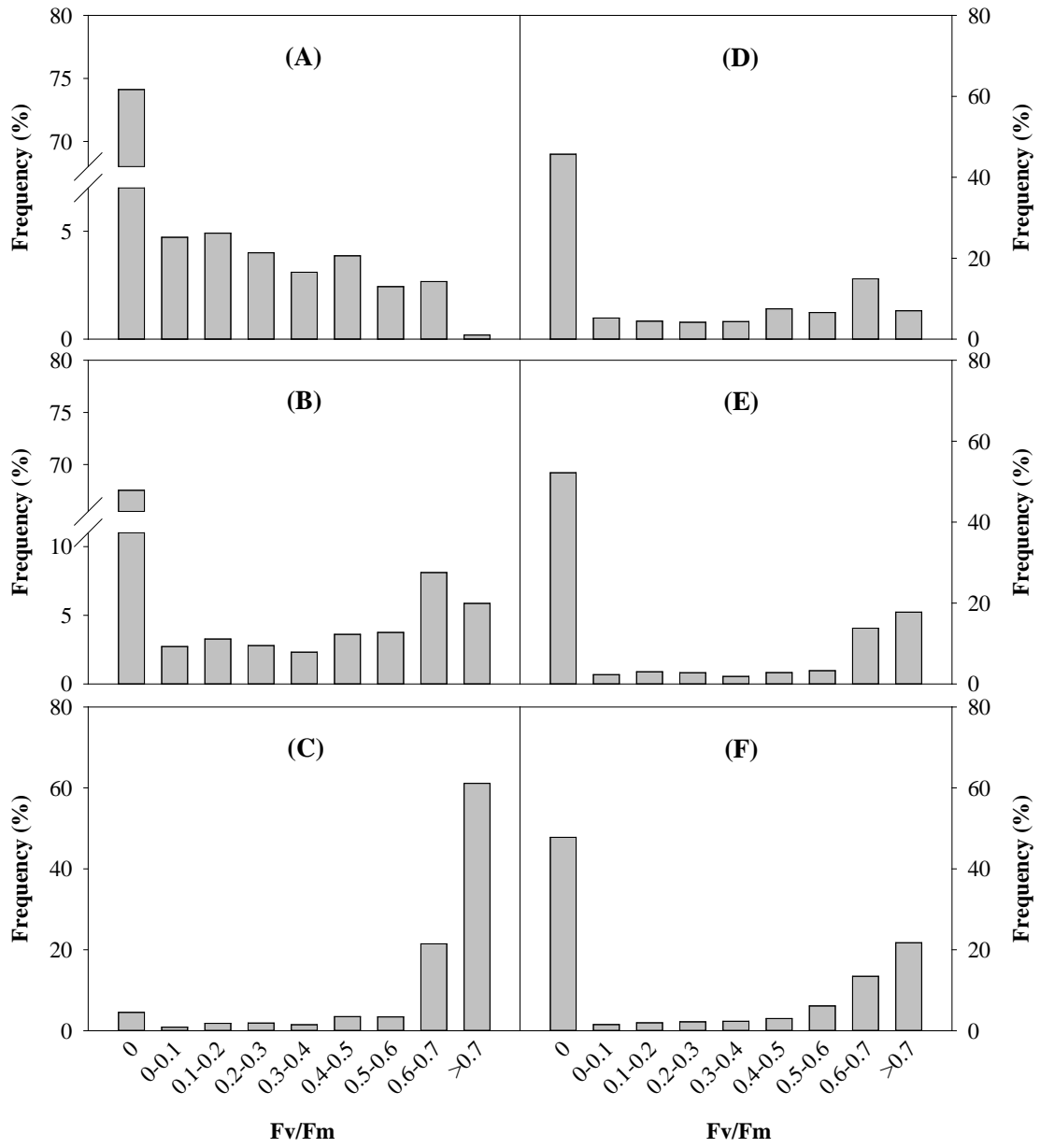
635

636

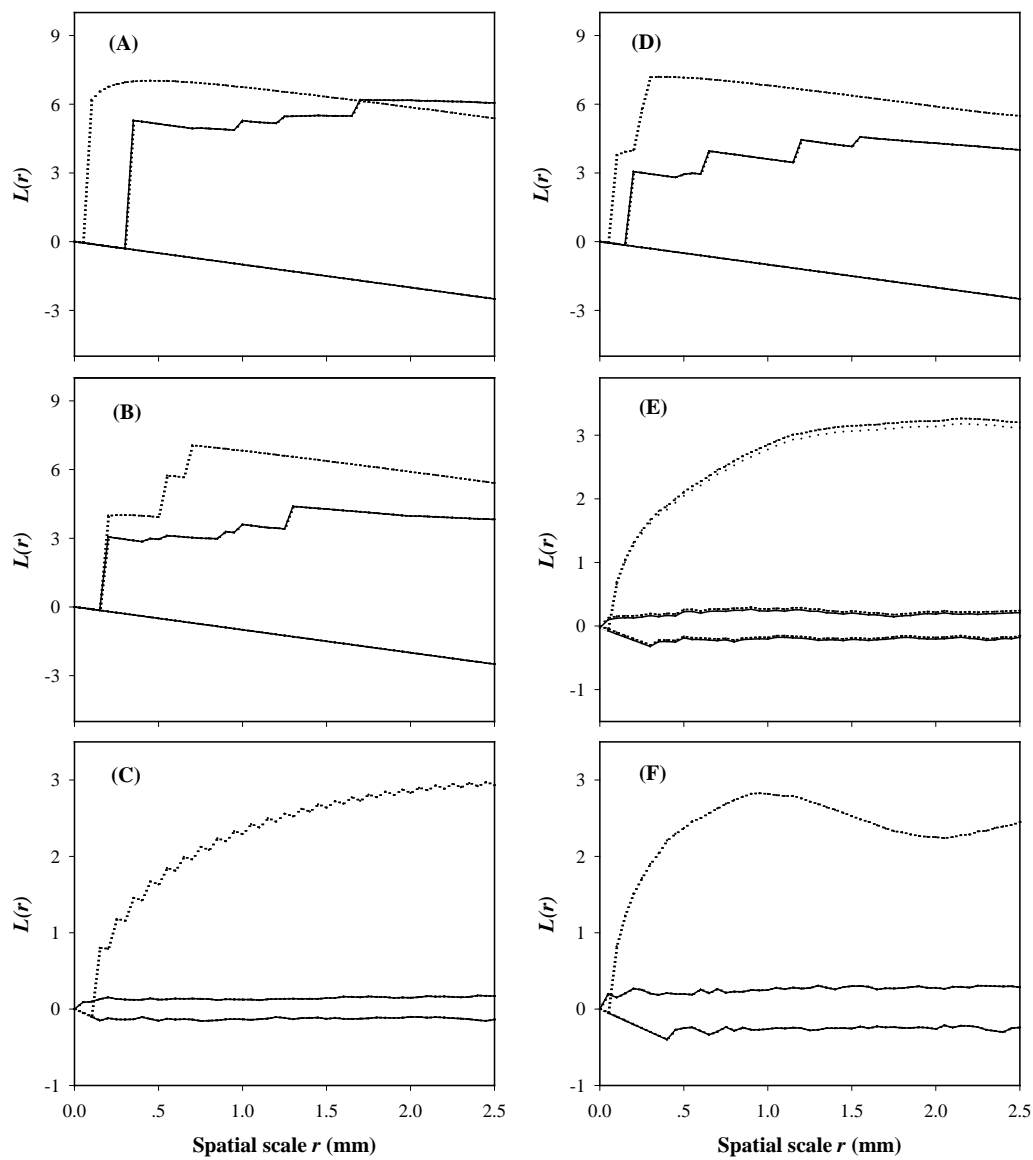
637

638

639 **Fig. 6**



640
 641
 642
 643
 644
 645
 646
 647
 648
 649



651
 652
 653
 654
 655
 656
 657
 658
 659
 660
 661

662 Table 1 Characteristics of the different successional stages of BSCs in the Shapotou region

Abbreviations	Crust successional stages	Dominant organisms	Crust color	Crust thickness (mm)	Cyanobacterial coverage (%)	Lichen coverage (%)	Moss coverage (%)
CSCs	Cyanobacterial (soil) crusts	<i>Microcoleus vaginatus</i>	Gray	2.93 ± 0.13	>97	0	<3
LSCs	Lichen (soil) crusts	<i>Collema</i> sp. (cyanolichen)	Black	7.44 ± 1.51	<27	>70	<3
MSCs	Moss (soil) crusts	<i>Bryum</i> sp.	Brown	14.62 ± 1.77	0	0	100
CLSCs	Cyanobacteria-lichen (soil) crusts	<i>M. vaginatus</i> and <i>Collema</i> sp.	Gray and black	5.72 ± 1.24	>67	<30	<3
CMSCs	Cyanobacteria-moss (soil) crusts	<i>M. vaginatus</i> and <i>Bryum</i> sp.	Gray and brown	6.18 ± 0.93	>70	0	<30
LMSCs	Lichen-moss (soil) crusts	<i>Collema</i> sp. and <i>Bryum</i> sp.	Black and brown	10.54 ± 1.18	<10	>40	<50

663

664

665

666

667

668

669

670

671

672

673

674

675

676

677

678

679

680

681

682

683 **Supplementary Material for:**

684 Small-scale spatial heterogeneity of photosynthetic fluorescence in biological soil crusts

685

686 Shubin Lan, Andrew David Thomas, Stephen Tooth, Li Wu, Chunxiang Hu*

687 * Corresponding author: Tel/Fax.: +86 27 68780866; E-mail address: cxhu@ihb.ac.cn

688

689 **This supplementary file includes 3 pages of information:**

690 Number of figures: 2

691

692

693

694

695

696

697

698

699

700

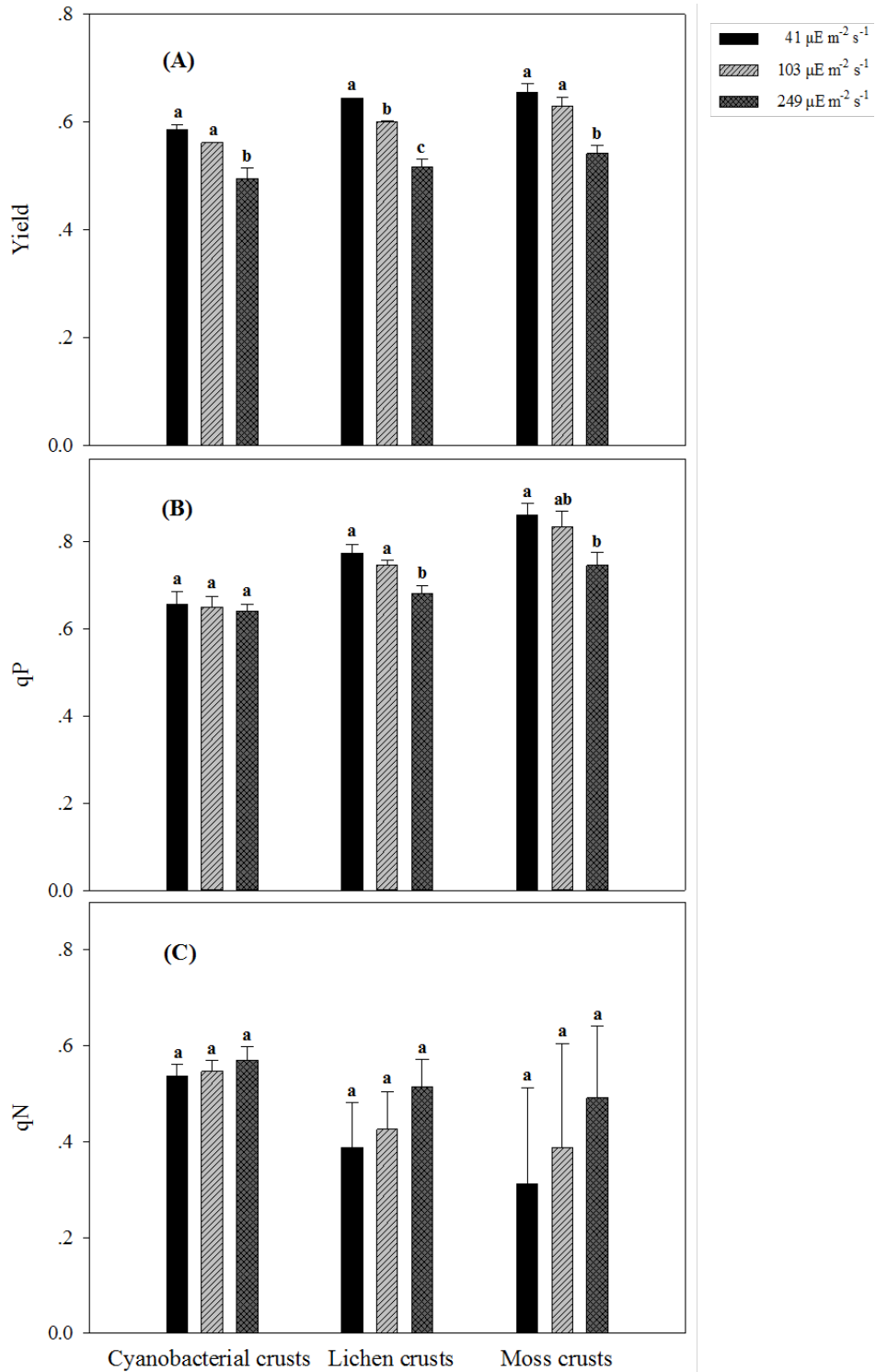
701

702

703



704 **Fig. S1** Comparison of three fluorescence parameters Yield (A), qP (B) and qN (C) under different actinic
 705 light conditions. For a crust sample, the values with different letters indicate the difference is significant at
 706 0.05 level ($P < 0.05$).

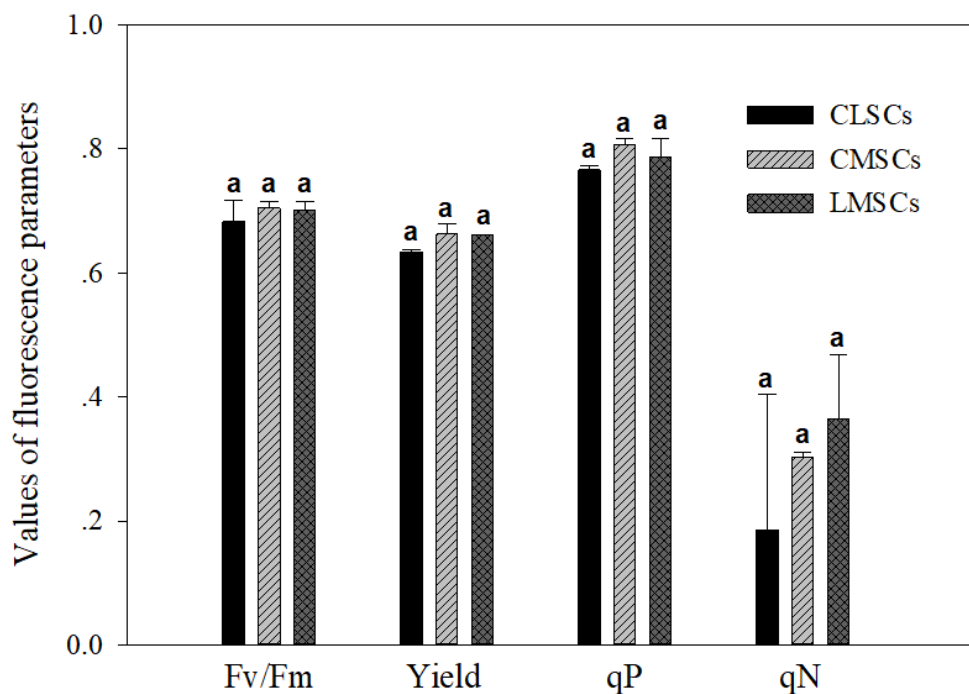


707

708

709

710 **Fig. S2** Comparison of fluorescence parameters Fv/Fm after dark adaptation and Yield, qP, qN under the
711 light condition of $41\mu\text{E m}^{-2} \text{s}^{-1}$. For each parameter, the values with same letters indicate the difference is
712 not significant at 0.05 level ($P>0.05$).



713
714
715
716
717
718
719